

# BURNING OF LAMINATED WOOD ASSEMBLY AFTER INTENSE HEAT EXPOSURE BY FIRE RESISTANCE FURNACE

Y. Saito<sup>1</sup>, K. Harada<sup>1</sup>, A. Sakaguchi<sup>2</sup>, K. Nakaue<sup>2</sup>, T. Tsuchihashi<sup>2</sup>, Y. Tanaka<sup>2</sup>, S. Tasaka<sup>2</sup> and M. Yoshida<sup>2</sup>

<sup>1</sup> Department of Architecture and Architectural Engineering, Kyoto University

<sup>2</sup> General Building Research Corporation of Japan

## ABSTRACT

To design timber elements to sustain not only during but also after fire, we need to know the burning behavior of timber elements. In this study, experiments were carried out to investigate the mechanism of burning during post heating period changing air supply rate for cooling. As the results, we got to know burning of wood dies out if the air supply rate is small. Additionally, numerical calculation model has been tried to develop to describe interaction between furnace condition and burning. However, the model did not predict the heat release rate accurately.

**KEYWORDS:** Fire resistance, Laminated wood assembly, Heat release rate, Post heat exposure, Air supply rate

## INTRODUCTION

Due to the movement toward environmental conscious, ecological society, use of natural wood products is being re-evaluated. In building construction, new technologies to build large-scale timber buildings are being desired. As to the seismic performance, well-designed timber structures behave sufficiently. However, fire performance of timber structure is in question. If fire spreads beyond compartment enclosures and structures fails to sustain load, part or whole building may collapse. In case of fire in large-scale timber buildings, structural integrity and load-bearing performance shall be examined carefully because structural collapse may lead to loss of life of occupants and as well as firefighters. In building design code in Japan, buildings with more than four stories shall not collapse by fire including cooling period of fire.

To prevent structural collapse during and after fire, structural elements are required to sustain applied load during and after fire. In case of timber structures, post heat behavior is extremely important. During fully-developed phase of fire, timber elements also burn. Even after fire, timber elements keeps on burning or smoldering. If self-burning continues for a long period, all the cross section is carbonated, which leads to collapse of elements and possibly whole structure.

There are many researches already carried out to predict the behavior of timber elements during heating phase.<sup>1-6</sup> However, knowledge is insufficient on the behavior during post heat exposure. For example, Konig *et al.*<sup>7</sup> carried out experiments including cooling phase of fire and tried to extend existing calculation method for heating phase. To apply to cooling phase behavior, they proposed to correct furnace temperature to effective furnace temperature in order to fit the calculated charring rate to experimental results. However, this model does not include the interaction between furnace environment and timber element. In reality, radiative heating effects by furnace walls and possibly by flame over specimen surface take a role to continue the self-burning. Consequently, it is difficult to predict cooling phase behavior using this type of modeling for universal conditions.

In the ISO834 fire resistance test<sup>8</sup>, it is said that post heating behavior is influenced by cooling conditions such as air supply rate, heat capacity of the furnace walls and so on. In this study, experiments were carried out to investigate the burning mechanism during post heating period. Using a small furnace, four experiments were carried out changing the air supply rate for cooling. The heat release rate (HRR, hereafter) from timber specimen and charring rate is compared between

experiments. Numerical calculation is being developed to describe the interaction between furnace condition and burning rate. As a first step, calculation results are demonstrated to show qualitative explanation of interaction between furnace environment and timber specimen.

## **EXPERIMENT**

### **Purpose of Experiments**

As described above, burning behavior during cooling period would be influenced by the method of cooling and furnace characteristics. However, in the present ISO834 fire resistance test procedure, air supply rate is not clearly determined. As a result, the burning behavior of timber elements may be altered by air supply rate and thermal inertia of furnace lining materials. In case of well-ventilated cooling, supplied air would move the heat away from furnace. This effect would result in rapid decrease furnace gas and wall lining temperatures. At the same time, supplied air would increase the burning rate of timber element. This effect will result in slow decrease of furnace gas and wall lining temperatures.

The adverse effect of supplying air in order to cool down the furnace is complicated and important problem. However, there are no measured data of burning rate in fire resistance test as far as we examined in published literatures. To examine the effect of air supply rate during cooling period, experiments were carried out changing air supply rate during cooling phase following ISO 834 standard heating. Temperature of furnace gas and specimen were measured. In addition, HRR of timber specimen was measured by the principle of oxygen consumption calorimeter. The influence of air supply rate to temperature and burning rate is discussed.

### **Experimental Apparatus**

A small-scale furnace was used for experiments as shown in Fig. 1. The furnace is cubic shaped (760 x 760 x 760 mm). Wall lining is made of ceramic-fiber board (thickness 150 mm, density 250 kg/m<sup>3</sup>). Specimen is equipped in one vertical position. The burner located on the opposing side of specimen. Premixed natural gas was supplied during heating phase. During cooling phase, natural gas was shutdown in order to supply only air to furnace.

Type K thermocouple was set in the center position 100 mm apart from specimen surface. Gas temperature was measured at every ten seconds. Gas sampling tube was set on one of the furnace wall 10mm apart from opening. Furnace gas was introduced to gas analyzer to measure oxygen, carbon dioxide and carbon monoxide concentrations at every five seconds.

On top surface, exhaust opening (57.4 cm<sup>2</sup>) is located. To measure air supply rate during cooling phase, pressure difference between inside of furnace and outside was measured. Effective flow area of opening was measured in advance by relating air flow velocity profile and furnace pressure at normal temperature. Using effective opening area, air supply rate was calculated by measured furnace pressure during experiments. At the same time, oxygen concentration was measured. Oxygen consumption was calculated by oxygen depletion and gas flow rate. Then the HRR of specimen was obtained by oxygen consumption.

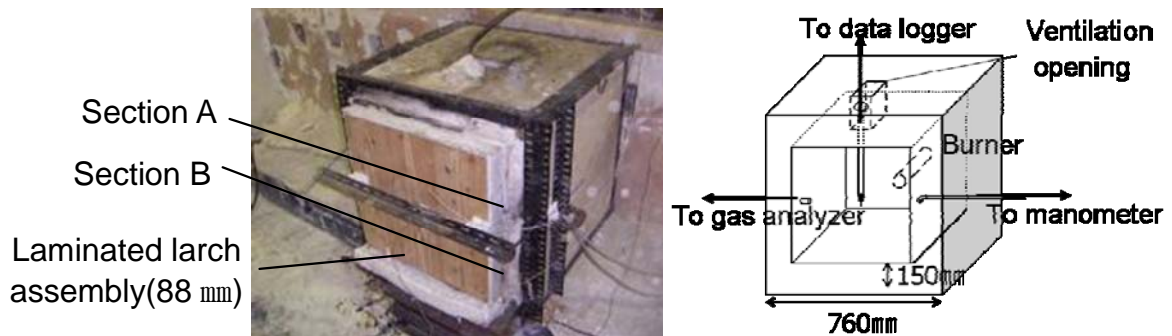


**FIGURE 1.** Experimental apparatus

### Specimen

Schematic of specimen is shown in Fig. 2. Specimen is a laminated larch wood assembly which consists of 12 laminar pieces (183.3 x 550 x 22 mm). Total width and height are 550 mm. Thickness is 88 mm. Ceramic-fiber is glued on specimen by 55 mm from four sides of specimen in order to prevent air leakage from the gap between the furnace walls and the specimen. Thus the effective exposed area is reduced to 440 x 440 mm on one side. In addition, thermocouples are embedded at three positions in the direction of thickness. As a result, thermocouple position is in accordance with bonding interface between each lamina. Another thermocouple is located at unexposed surface as specified by ISO 834.

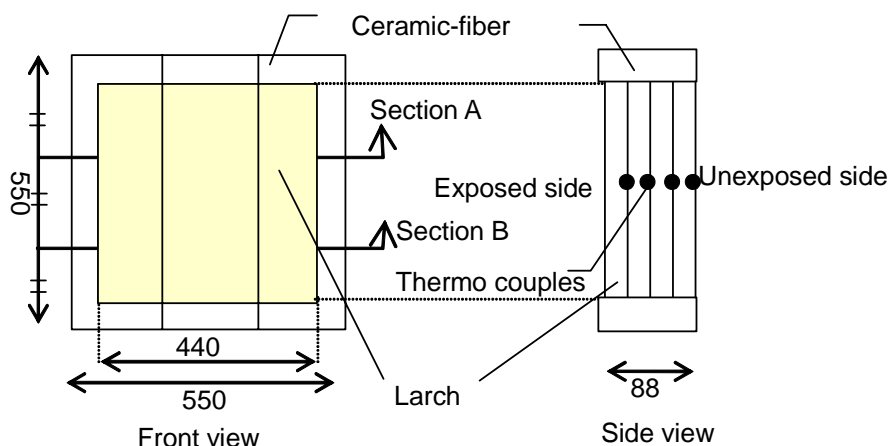


**FIGURE 2.** Specimen

### Experimental Procedure

Four experiments were carried out. For the first one hour, specimen was heated in accordance with ISO 834 standard fire temperature. After one hour of heating, air is supplied to furnace in order to cool down the furnace and specimen. Cooling was continued for 3 hours. Air supply rate was changed between experiments. Experimental conditions are shown in Table 1. In three of the experiments (S, M, L), specimens are cooled down as it was fixed in the furnace. In one of the experiments (N), specimen was removed from furnace immediately after heating and cooled down in quiescent air.

For three hours after heating, burring behavior was observed and recorded by VTR camera. After three hours, specimens are extinguished by water if it was still burning. Then the specimen was cut by electric saw along sections A and B to measure charred depth.

**TABLE 1.** Experimental conditions

Symbol	Method of cooling	air supply rate per unit exposed surface of specimen (kg/s·m <sup>2</sup> )
S	Cooled as fixed to furnace (forced ventilation)	0.041
M		0.06
L		0.119
N	removed from furnace immediately after heating	(cooling by natural convection)

## Results and Discussion

### 1) Furnace temperature

Experimental results are shown in Figs. 3 to 10. The results of furnace gas temperature are shown in Fig. 3. Heating temperature (0 to 60 minutes) is common to all the tests. At 60 minutes, supply of fuel gas is stopped. After that, only air was supplied to furnace as specified in Table 1. Soon after stop of heating, furnace gas temperature decreases rapidly. Comparing between tests S, M and L, furnace temperature during first several minutes of decay (60 to 70 minutes) is lower as air supply rate is larger. In this period, supplied air mainly works to expel hot gas from furnace. After 70 minutes, cooling rate is reduced in test L. This implies that burning of specimen would release heat to furnace. As a result, furnace temperature in test L is higher than test M after 75 minutes. After 170 minutes, furnace temperature in test L is the highest among all the tests. As was demonstrated, supplied air works as oxidizer to enhance combustion during later stage of cooling.

### 2) Heat release rate and burning behavior

HRR of specimen is shown in the Fig. 4 along with visual observations during tests. In all experiments, HRR is about 60 kW/m<sup>2</sup> (per unit exposed surface area) at the moment of stop of heating. Then HRR is rapidly decreased. The degree of decrease depends on air supply rate. In case of test S, HRR is rapidly decreased to 4 kW/m<sup>2</sup> at 78 minutes. After that, HRR gradually decreased. At 100 minutes, flaming combustion at surface is stopped. Then HRR is further decreased toward zero (extinction). In contrast, HRR in test L was kept to a certain magnitude. After 70 minutes, measured HRR values fluctuate. This is because of intense burning of surface. Even after the stop of flaming at 85 minutes, specimen surface glowed. As the char layer depth is increased, small pieces of char would fall down. Then “new” surface is created to increase HRR. This process is repeated on and on. At 190 minutes, large piece of char layer would fall down to drastic increase of HRR. In case of test M, the overall tendency is close to test S.

Comparing burning behavior between tests, spill flame out of ventilation opening stopped at 70 minutes in test S, at 65 minutes in test M and at 61 minutes in test L. Duration of spill flame tends to be longer as air supply rate is reduced. Flaming of specimen surface stopped at 100 minutes in test S, at 85 minutes in test M, and at 83 minutes in test L. Similar to spill flame, duration of surface flaming tends to be longer as air supply rate is reduced.

### 3) Specimen temperature

The temperatures at 22mm from exposed surface are shown in Fig. 5. The temperatures of test S and L were almost the same, but temperature of test M was lower than the other two tests. The reason for this difference was still under consideration. Temperature of test N decreased rapidly, because heat could quickly be transferred to surrounding air.

The temperatures at 44mm from exposed surface are shown in Fig. 6. The temperature of tests S, M

and L continued to increase after heating. After 200 minutes, the temperature in test L gradually decreased because charring front had passed through temperature measuring point. The temperature of test N rapidly decreased similar to the position of 22 mm from exposed surface.

The temperatures at 66 mm from exposed surface are shown in Fig. 7. The temperature of test L increases up to 180 minutes when charring front went through. Sharp peak can be seen in the plot of test L. In other tests, temperature history has no distinct peak, but tends to decrease. This tendency is similar in unexposed surface temperatures as shown in Fig. 8. The temperature of test L tends to be increased towards burning temperature. The temperature of tests S and M were almost the same. The temperature of test N is the lowest.

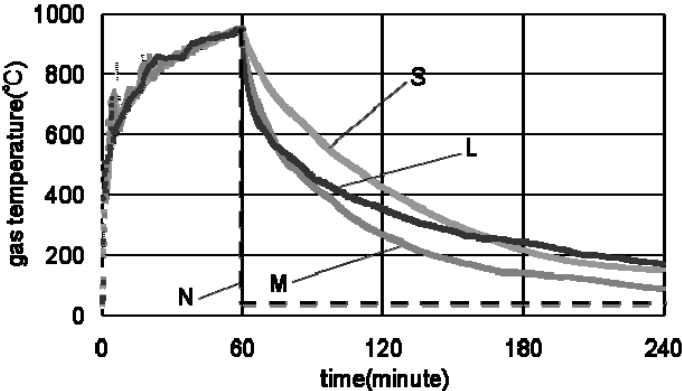


FIGURE 3. Furnace gas temperature

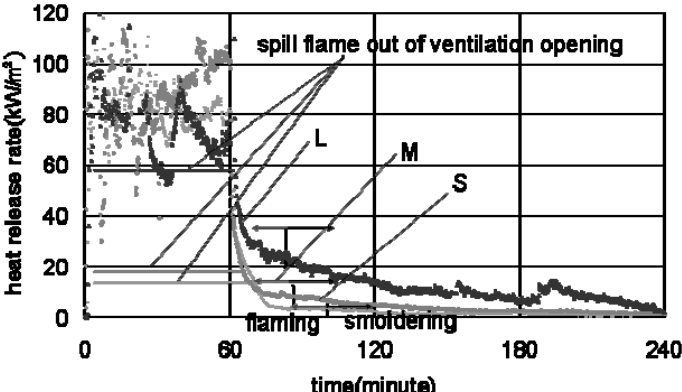


FIGURE 4. HRR per unit exposed surface area of specimen

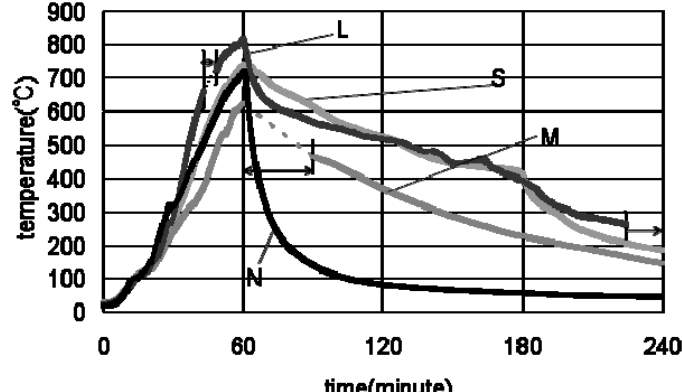


FIGURE 5. Specimen temperature at 22mm from exposed surface

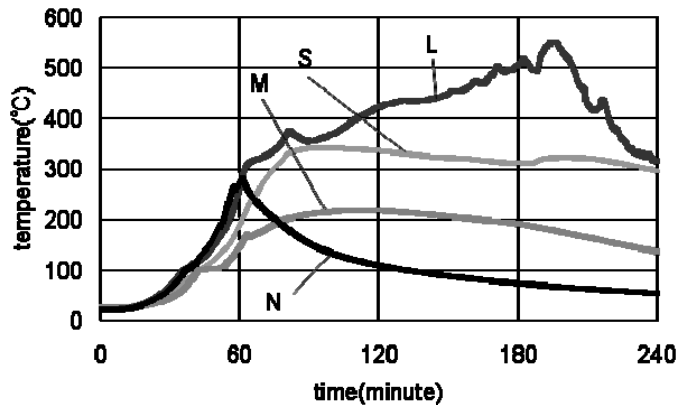


FIGURE 6. Specimen temperature at 44mm from exposed surface

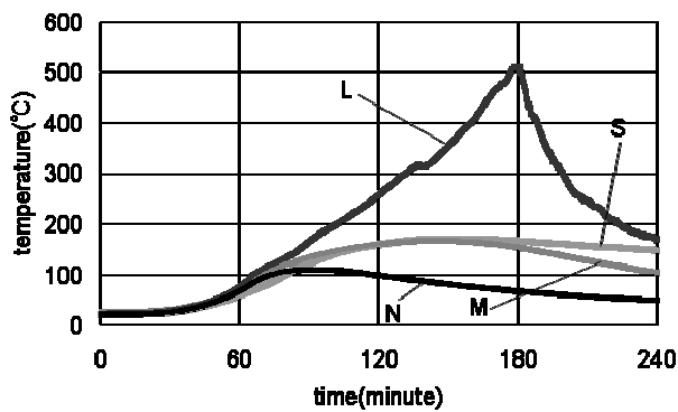


FIGURE 7. Specimen temperature at 66 mm from exposed surface

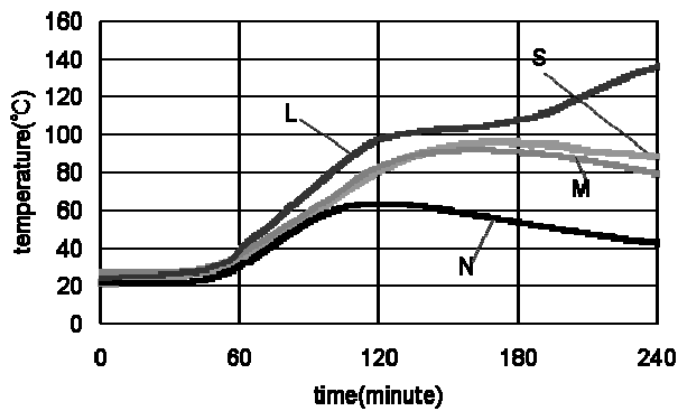


FIGURE 8. Specimen temperature at unexposed surface

4) Charred layer observed after heating

At 240 minutes, all the tests were terminated. Specimens were subjected to visual observation. It was confirmed that specimens S and M had already stopped burning. Even though very slow, specimen N was still burning. Specimen L was burning slightly.

All the specimens were cut by saw to measure charred depths. The photographs of cross-section are shown in Fig. 9. Measured charred depths are shown in Table 2. Comparing specimens S, M and L, charring depth is large as air supply rate is increased. Charring depth of N was the smallest of all the

experiments. Except for S, char depths were the difference between section A and Section B.

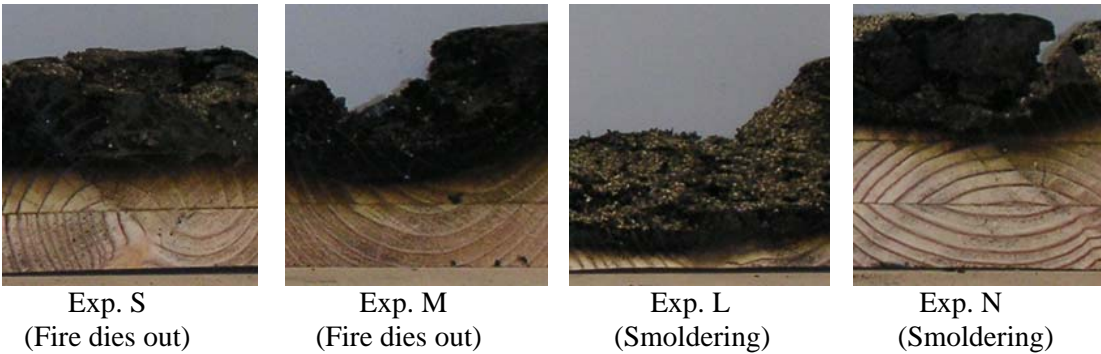


FIGURE 9. Photographs of cross-section after experiment

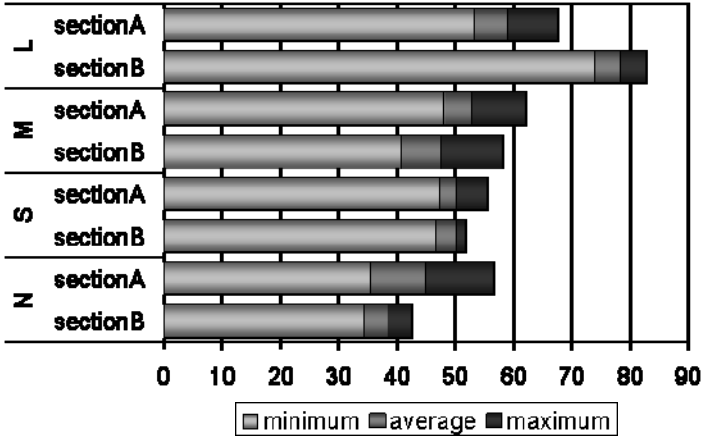


FIGURE 10. Charred depth

**Summary of Experimental Findings**

In summary of experimental results, it was found that

- a) HRR is increased as air supply rate is increased, if specimen is cooled as fixed to furnace,
- b) charred depth is also increased as air supply rate is increased,
- c) self extinction was observed in the conditions of small air supply rate
- d) If specimen is detached from furnace soon after heating, charred depth and specimen temperature are reduced. However, slow burning continues.

**NUMERICAL CALCULATIONS**

**Purpose of Numerical Calculations**

As was demonstrated, burning behavior of timber specimen is complicated. To understand the mechanism, a simple model was developed to describe the behavior during initial heating up to self-burnout. In order to consider interaction between heating condition and burning, mathematical model was developed. Calculated results were compared with experimental results.

## Heat Transfer in Furnace

Heat transfer in the furnace is shown in Fig. 11. The heat released by flaming combustion is added to the energy balance of furnace gas. The heat released by smoldering combustion was once absorbed by charred layer. Part of the heat is released to furnace side, but the rest is conducted towards wood specimen. Radiation and convection heat transfer between furnace gas, specimen surface and furnace wall surface are considered. To account for the effect of ventilation, enthalpy flow to and from outside air was also considered.

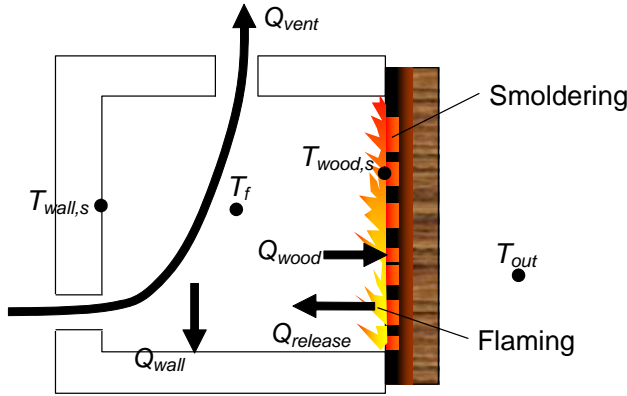


FIGURE 11. Heat transfer in the furnace

## Description of the Analytical Model

This model is able to calculate HRR by solving furnace heat balance equation and one-dimensional heat conduction equation of wood specimen and furnace wall simultaneously. Furnace heat balance was calculated considering heat released by flaming combustion, heat loss due to ventilation and heat absorption by furnace walls and wood specimen. However, it was difficult to calculate HRR by smoldering combustion. Thus a fixed value ( $6 \text{ kW/m}^2$ ) was applied.

Radiation in the furnace was solved by interreflection simultaneous equations. Furnace heat balance was expressed as:

$$C_p \rho V \frac{\partial T_f}{\partial t} = Q_{\text{release}} - Q_{\text{vent}} - Q_{\text{wood}} - Q_{\text{wall}} \quad [1]$$

where  $\rho$  is furnace gas density ( $\text{kg/m}^3$ ),  $C_p$  is furnace gas specific heat ( $\text{J/kg}\cdot\text{K}$ ),  $V$  is furnace gas volume ( $\text{m}^3$ ), and  $T_f$  is furnace gas temperature ( $^\circ\text{C}$ ). Rate of heat loss by ventilation  $Q_{\text{vent}}$  can be expressed as:

$$Q_{\text{vent}} = GC_p (T_f - T_{\text{out}}) \quad [2]$$

where  $G$  is air supply rate ( $\text{kg/s}$ ). The HRR by flaming combustion  $Q_{\text{release}}$  can be expressed as:

$$Q_{\text{release}} = -\Delta H \frac{dW}{dt} = -\Delta H \int_V \rho_o \frac{\partial R(T_{\text{wood}})}{\partial T_{\text{wood}}} \frac{dT_{\text{wood}}}{dt} dV \quad [3]$$

where  $\Delta H$  is heat of combustion per unit weight of wood ( $\text{kJ/kg}$ ),  $W(t)$  is specimen weight at time  $t$ ,  $\rho_o$



is dry density of wood ( $\text{kg/m}^3$ ) and  $R$  is residual ratio as a function of specimen temperature.

Heat conduction of furnace walls and specimen is expressed by one-dimensional heat equation. Latent heat of water evaporation and heat of decomposition of wood species were considered. The one-dimensional heat conduction equation is expressed as:

$$C_{wood} \rho_{wood} \frac{\partial T_{wood}}{\partial t} = \frac{\partial}{\partial x} (\lambda_{wood} \frac{\partial T_{wood}}{\partial x}) - Q_{decomp} - Q_{evap} \quad [4]$$

## Material Properties

In calculations, material properties are selected as shown in Table \*.

**TABLE \*** List of material properties and experimental conditions

Item	symbol	value
(wood specimen) specific heat	$C_{wood}$ (J/kg·K)	$-213 + 4.87(T_{wood} + 273)$
density	$\rho_{wood}$ ( $\text{kg/m}^3$ )	560
thermal conductivity	$\lambda_{wood}$ (W/m·K)	$(0.0257 + 0.000196\rho_0) \times (T_{wood} + 273) / 2$
specimen thickness	$l_{wood}$ (m)	0.088
exposed area	$A_{wood}$ ( $\text{m}^2$ )	0.1936
Emissivity	$\varepsilon_{wood}$ (-)	0.7
dry density	$\rho_0$ ( $\text{kg/m}^3$ )	500
heat of combustion	$\Delta H$ (kJ/kg)	16000
heat of decomposition	$L_v$ (J/kg)	$3.59 \times 10^6$
latent heat of water evaporation	$L_w$ (J/kg)	$2.258 \times 10^6$
(Charred layer) specific heat	$c_{char}$ (J/kg·K)	$0.54c_{wood}$
thermal conductivity	$\lambda_{char}$ (W/m·K)	0.18
emissivity	$\varepsilon_{char}$ (-)	1
(furnace wall: ceramic fiber board) specific heat	$C_{wall}$ (J/kg·K)	$1.13 \times 10^3$
density	$\rho_{wall}$ ( $\text{kg/m}^3$ )	250
thermal conductivity	$\lambda_{wall}$ (W/m·K)	$0.00125T_{wall}^2 + 0.0025T_{wall} + 0.06$
wall thickness	$l_{wall}$ (m)	0.15
surface area	$A_{wall}$ ( $\text{m}^2$ )	1.058
Emissivity	$\varepsilon_{wall}$ (-)	0.9
(furnace heat transfer) ambient air temperature	$T_{out}$ ( $^{\circ}\text{C}$ )	23.0
emissivity of furnace gas	$\varepsilon_f$ (-)	0.2
specific heat of furnace gas	$C_p$ (J/kg·K)	$1.007 \times 10^3$ (300K) $1.142 \times 10^3$ (1000K)
density of furnace gas	$\rho_{air}$ ( $\text{kg/m}^3$ )	$353/(T_f + 273)$
air supply rate	$G$ (kg/s)	0.00797(S) 0.0117(M) 0.023(L)

## Comparison of Calculations and Experiments

Comparisons of experimental results and calculated results are shown in Figs. 12 to 14. The furnace gas temperature is shown in Fig. 12. All calculated furnace gas temperatures decrease rapidly after 60 minutes. Calculated values were smaller than the experimental measurements. However, the overall pattern of change could be reproduced qualitatively. The quantitative discussion will be in future development, however ventilation heat loss by air supply strongly affect furnace gas temperature during cooling phase. Calculation may take the effect excessively.

The calculation result of HRR is shown in Fig. 13. Similar to the comparison of gas temperature, all calculated HRR values were smaller than the experiments. Calculated values were about 40 % of experimental measurements. In the experiments, HRR was increased as air supply rate is increased. However, in calculation, HRR is reduced as air supply rate is increased. At present model, increase of smoldering (glowing) HRR by air flow is not taken into account, thus the increase of air supply simply decrease the furnace temperature and as well as HRR by flaming combustion.

The specimen temperature at 22 mm from the exposed surface is shown in Fig. 14. In all the calculations, temperatures were considerably lower than the experimental values.

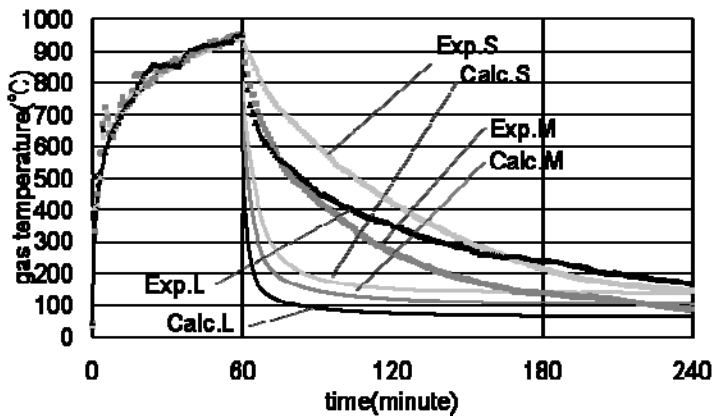


FIGURE 12. Gas temperature – Comparison of experimental results and calculation results

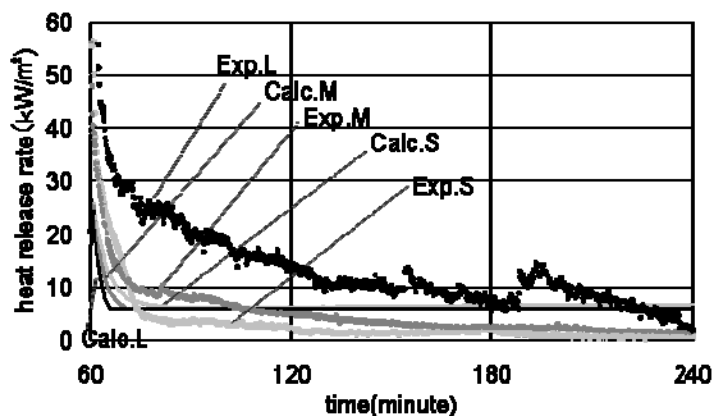
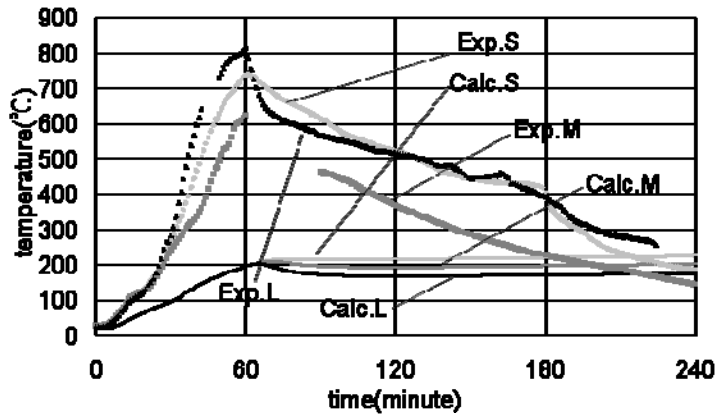


FIGURE 13. HRR per unit exposed area of wood – Comparison with experiments



**FIGURE 14.** Specimen temperature at 22 mm from the exposed surface – Comparison with experiments

### Summary of Numerical Calculations

A numerical calculation method was developed to account for interactions between furnace environment and burning behavior of specimen. At present the model is not sufficient, however the followings are pointed out.

- a) By coupling furnace heat transfer and heat conduction in specimen, it would be promising to predict overall behavior of wood specimen after heating.
- b) At present, interaction between air supply and smoldering (glowing) combustion, falling out of charred layer to show “new” surface are not introduced. These factors would have to be considered for accurate predictions.

### CONCLUSIONS AND FUTURE DEVELOPMENTS

In this study, ISO 834 fire-resistance tests were carried out to investigate the burning behavior of laminated larch assembly during cooling phase. By changing air supply rate for cooling, it turned out that the smoldering combustion is self-stopped if the air supply rate is small. In case of excess air supply, burning is activated to raise furnace temperature and increase damage of specimen.

To predict the burning behavior during cooling phase, a numerical model was developed. As a preliminary investigation, calculations were carried out to simulate the experiments. By examining the discrepancies between experiments and calculations, it was pointed out that further development of model is needed to include glowing combustion, drop of charred layer and so on.

### REFERENCES

1. Takeda, H. and Mehaffey, J.R., “A Model for Predicting Heat Transfer”, *Fire And Materials*, 22, 133-140, 1998.
2. Richarson, Leslie R., “Thought and Observation on Fire-Endurance Tests of Wood-Flame Assemblies Protected by Gypsum Board”, *Fire and Materials*, 25, 223-239, 2001.
3. Clancy, P. and Young, S.A., “Full Experiments for Evaluating Theoretical Fire Wall Models”, *Fire and Materials*, 28, 431-458, 2004.
4. Collins, G.E., Collier, P.R.C. and Mackenzie, C.E., “Fire Resistance of Timber-Framed Floors and Walls”, Technical Report 93/5, pp. 1-25, 1993.11.
5. Yasui, N., Shimizu, M., Hasemi, Y., Kamijima, M., Kimura, T., Hokugo, A., Tamura, Y., Yoshida, M. and Yamamoto, K., “Prediction and Design of Mechanical Fire Resistance of Japanese

- Traditional Wood/Soil Walls by Compression Tests of Wood Posts”, J. Environ. Eng., Architectural Institute of Japan, 574, 1-6, 2003. (In Japanese)
6. Konig, Jurgan, “Effective Thermal Actions and Thermal Properties of Timber Members in Natural Fires”, Fire and Materials, 30, 51-63, 2006.
  7. International Organization for Standardization, ISO 834 Fire Resistance Test – Methods of Construction, 2000.